Design of a Crossflow Attenuated Natural Laminar Flow Flight Test Article

Michelle N. Lynde[1], Richard L. Campbell[2], and Brett R. Hiller[3]
NASA Langley Research Center, Hampton, Virginia, 23681

This abstract includes preliminary information on the computational design and analysis of a flight test article. The flight test aims to experimentally validate the new Crossflow Attenuated Natural Laminar Flow (CATNLF) design method in a flight environment. The CATNLF design method uses geometry shaping to produce specific pressure distributions that enable laminar flow on vehicle components with high sweep and high Reynolds numbers by attenuating the crossflow growth that typically leads to premature transition on such components. The flight test article design is scheduled to be completed at the end of 2019, with model fabrication beginning in early 2020. Design results presented in this abstract are representative of the final test article. The final paper will be updated to include the finalized test article geometry and analysis.

Nomenclature

Acronyms

BLSTA3D	=	Boundary Layer code for Stability Analysis 3D, boundary layer profile solver
CATNLF	=	Crossflow Attenuated Natural Laminar Flow
CDISC	=	Constrained Direct Iterative Surface Curvature, design module
CF	=	Crossflow
CLIP	=	Centerline Instrument Pylon
CRM-NLF	=	Common Research Model with Natural Laminar Flow
DRE	=	Distributed Roughness Elements
FATCAT	=	Flight Article Test for Crossflow Attenuation
FC	=	Full Configuration
ITA	=	Isolated Test Article
LASTRAC	=	Langley Stability and Transition Analysis Code, transition prediction software
LFC	=	Laminar flow control
LST	=	Linear Stability Theory
NASA	=	National Aeronautics and Space Administration
NLF	=	Natural laminar flow
NTF	=	National Transonic Facility
RANS	=	Reynolds-Averaged Navier-Stokes
ReHEAT	=	Resistive Heating for the Evaluation of Aerodynamic Transition
TS	=	Tollmien-Schlichting
USM3D	=	Unstructured Mesh 3D, Navier-Stokes flow solver

Symbols

α_{ITA}	=	Angle of attack of the test article
β_{FC}	=	Angle of sideslip of the full configuration
c	=	Chord length
C_P	=	Pressure coefficient
M	=	Mach number
Re_θ	=	Reynolds number based on attachment line boundary layer momentum thickness

[1] Research Aerospace Engineer, NASA Langley Research Center, Mail Stop 499, Hampton, VA 23681, AIAA Member.
[2] Senior Research Engineer, NASA Langley Research Center, Mail Stop 499, Hampton, VA 23681, AIAA Associate Fellow.
[3] Research Aerospace Engineer, NASA Langley Research Center, Mail Stop 499, Hampton, VA 23681, AIAA Member.

Re'	=	Unit Reynolds number
Re$_{MAC}$	=	Reynolds number based on mean aerodynamic chord
x/c	=	x-location nondimensionalized by local chord
z/c	=	z-location nondimensionalized by local chord

I. Introduction

AVIATION has developed into a strong industry over the last century, with particularly rapid growth over the previous few decades due in part to a booming commercial market and increased demand for air cargo capabilities. Current market projections suggest air traffic will continue to grow by approximately 4.6% over the next 20 years, inspiring the aviation industry to develop next-generation aircraft to accommodate this anticipated growth [1]. Increased environmental awareness has led to ambitious performance goals for these next-generation aircraft in order to make the projected air travel demands compatible with new ecofriendly regulations. Objectives for Green Aviation, including increased fuel efficiency, lower emissions, and reduced noise, have motivated technological research and development of promising concepts that may help reach these performance goals. One such technology being investigated is the implementation of laminar flow, which offers the potential to increase fuel efficiency by significantly reducing aircraft drag via lower skin friction and profile drag. Laminar flow technology has been researched since the 1940s with various successful, yet limited, applications. Recently, laminar flow has begun making its way onto modern commercial aircraft on components such as the nacelles, winglets, fuselage, and low-swept wings [2, 3]. While these existing applications of laminar flow have proven to reduce aircraft drag, one of the greatest potential for performance improvements due to laminar flow is its implementation on the wings of typical commercial transports. The main wings have been a challenge for applications of laminar flow primarily due to the rapid growth of crossflow instabilities that occurs on components with high sweep or Reynolds numbers. Most modern commercial transports have highly swept wings in order to meet cruise speed requirements. Historic techniques to address transition due to crossflow instabilities include a laminar flow control (LFC) system or a reduction in wing sweep. A LFC system, such as suction, often increases the complexity, cost, and weight of the vehicle, which has limited the application of LFC systems on commercial transports. A reduction in wing sweep inherently requires an often undesirable reduction in the cruise speed of the vehicle. A more recent technology, distributed roughness elements (DREs), has demonstrated some success in reducing crossflow instabilities, but inconsistent flight test results have required additional fundamental research before any commercial application is feasible [4].

A new laminar flow technology, referred to as Crossflow Attenuated Natural Laminar Flow (CATNLF), has been developed to reduce the growth of crossflow instabilities on components with high sweep and Reynolds numbers. The CATNLF method utilizes airfoil geometry shaping to obtain specific pressure distributions that are known to reduce crossflow growth to a subcritical level in the leading-edge region of a wing. This method has been applied in computational studies to both transonic and supersonic commercial transports [5, 6]. The CATNLF method was employed in the design of a wind tunnel model, referred to as the Common Research Model with Natural Laminar Flow (CRM-NLF), which was tested in the National Transonic Facility (NTF) at the NASA Langley Research Center (LaRC) to experimentally validate the computational predictions of the technology [7]. Experimental results from the wind tunnel test showed significant extents of laminar flow at transonic cruise speeds, as well as good agreement between the experimental data and computational predictions of laminar flow regions [8, 9, 10]. The wind tunnel test has led to the AIAA Transition Prediction Workshop using the CRM-NLF as a test configuration for workshop participants, highlighting the current industry interest in practical laminar flow applications. Figure 1 compares the maximum extent of laminar flow, measured in transition Reynolds number, of a variety of natural laminar flow (NLF) experiments originally compiled by Malik et al. [11]. This plot illustrates the relatively large extents of laminar flow seen on the CRM-NLF in the NTF compared to historic NLF experiments on components with comparable sweep, alluding to the success of the CATNLF method in reducing the crossflow growth on highly swept wings.
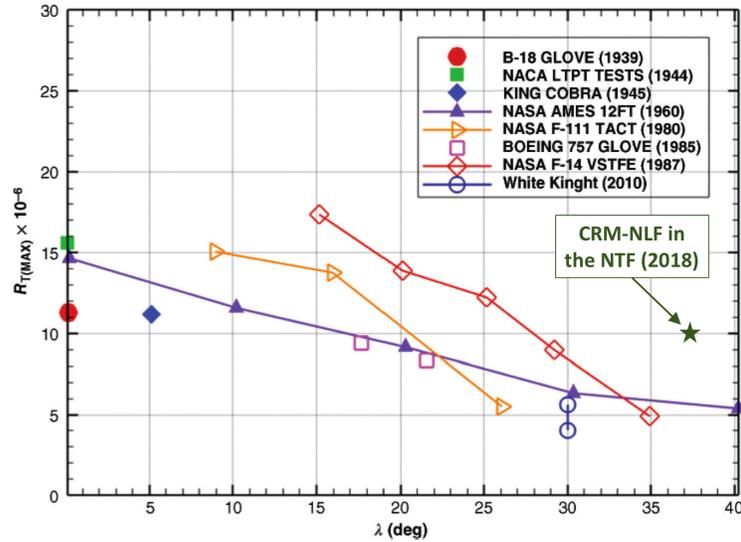
Figure 1. Data compiled by Malik et al. [11] that compares several NLF experiments with CRM-NLF test in the NTF overlaid on the original plot.

While the CRM-NLF wind tunnel test in the NTF provided preliminary experimental confirmation of the CATNLF technology, challenges during the experimental investigation limited the test conditions at which high-quality data could be acquired. Extents of laminar flow are strongly dependent on environmental factors, such as freestream turbulence levels, and can be limited by bypass transition due to surface imperfections. These environmental factors and bypass transition are typically more detrimental to the extent of laminar flow in a wind tunnel environment compared to a flight environment. This is primarily because the freestream turbulence levels are usually higher in a wind tunnel, and the increased unit Reynolds number in a wind tunnel makes smaller surface imperfections critical, leading to additional bypass transition. During the CRM-NLF test in the NTF, the extents of laminar flow at the high Reynolds number test conditions (i.e., Re_{MAC} > 20 million) were limited by bypass transition. This high Reynolds number limitation led to the proposal of a flight test series to experimentally validate the CATNLF method in a flight environment, which includes lower turbulence levels, as well as unit Reynolds numbers closer to that seen on a transonic transport. The upcoming flight test series is a collaborative effort between researchers and engineers at the NASA Langley Research Center and the NASA Armstrong Flight Research Center. It is comprised of three flight tests, all of which will be flown on an existing flight testbed at Armstrong Flight Research Center known as the Centerline Instrument Pylon (CLIP) underneath an F-15 aircraft. This flight testbed has been successfully used for laminar flow experiments previously [12]. The first of three flight tests in the series, referred to as Resistive Heating for the Evaluation of Aerodynamic Transition (ReHEAT), is to validate an experimental test technique that will improve the efficiency and quality of the laminar flow visualization data acquired during the flight test series. ReHEAT was completed in 2019 and preliminary results from the flight test are scheduled to be published at AIAA Aviation 2020 in a separate paper. The second flight test, referred to as Flow Rake, will gather essential information about the flow quality beneath the F-15, including local conditions and turbulence levels, and is tentatively scheduled to fly in 2020. The final flight test, referred to as Flight Article Test for Crossflow Attenuation (FATCAT), will be used to evaluate the CATNLF technology in a flight-relevant environment. The test article used in the final flight test will be designed using the CATNLF method to delay transition at transonic cruise speeds on high sweep, high Reynolds number components. The FATCAT test article is planned to be used to accomplish two primary goals: first, to confirm the effectiveness of the CATNLF method in attenuating crossflow growth on a representative transonic transport wing, and second, to investigate surface requirements needed at transport-relevant unit Reynolds numbers.

This abstract documents the computational design and analysis of the FATCAT flight test article, including information on the computational tools, transition delay method, design conditions, preliminary airfoil geometry and pressure changes, predicted extents of laminar flow, and details of the flight test strategy. The final design of the test article is scheduled to be completed by the end of 2019, with manufacturing beginning soon after. The updated final design results, as well as off-design analysis of the test article, will be included in the final paper.

II. Design and Analysis Approach

The aerodynamic design of the FATCAT flight test article was performed using a suit of computational tools with the goal of obtaining significant extents of laminar flow at the cruise design condition. This subsection will present the computational tools employed in the design and analysis process, as well as a brief description of the CATNLF boundary layer transition delay method.

A. Computational Tools

Several computational tools were used during the aerodynamic design and analysis of the FATCAT test article, including a flow solver, design code, and transition prediction software. The work flow of the computational tools is illustrated in Figure 2. The flow solver chosen for this work, USM3D [13], is a Reynolds-Averaged Navier-Stokes (RANS) solver that uses unstructured tetrahedral grids. This flow solver was coupled with the design code to determine the shape of the FATCAT test article. The design code used is a knowledge-based inverse design tool, CDISC [14], which has been used in many aerodynamic design projects including computational studies, wind tunnel models, and flight test efforts. For transition prediction, a boundary layer profile solver, BLSTA3D [15], was used to calculate the velocity and temperature profiles from the flow solver pressure distributions. These boundary layer profiles are used in LASTRAC [16], the stability analysis code, to calculate the growth of both Tollmien-Schlichting (TS) and crossflow (CF) modal instabilities and estimate the extents of laminar flow on the flight test article. All stability analysis calculations are based on Linear Stability Theory (LST) with compressibility effects included. The final paper will include additional detail about each computational tool employed in this effort.
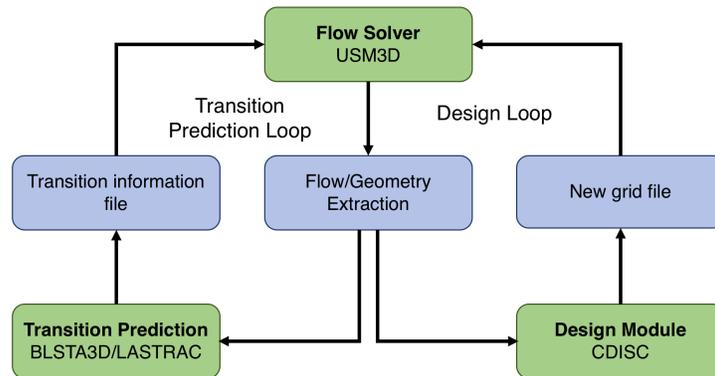

Figure 2. Flow chart for the computational tools employed in this aerodynamic design work.

B. Crossflow Attenuated Natural Laminar Flow (CATNLF) Design Method

The CATNLF transition delay method aims to enable significant extents of laminar flow on wings with high sweep and Reynolds number, such as those on traditional transonic transports, that have previously been limited by crossflow transition. The strategy used to suppress the crossflow growth in the leading-edge region, as well as control the midchord Tollmien-Schlichting transition location, is to introduce unique pressure distribution architecture. The CATNLF method of transition delay was developed in computational studies [6, 7] and experimentally investigated in a wind tunnel test in 2018 [7, 8, 9, 10].

A sample CATNLF pressure distribution for a transonic wing is shown in Figure 3 with several key features highlighted. The rapid acceleration near the leading edge is the primary mechanism for keeping the crossflow growth subcritical. A pressure gradient tailored to control Tollmien-Schlichting growth is introduced between the end of the rapid acceleration region and the desired chordwise transition location. Figure 4 shows the CF and TS N-factor growth for the sample CATNLF pressure distribution from Figure 3. The character shown in the N-factor growth plots are representative of those seen on typical CATNLF wings. The CF grows rapidly over a short region near the leading edge, reaches a subcritical maximum value, and then damps over the remainder of the chord. The TS growth is designed to slowly increase from the leading edge to the desired chordwise transition location. These N-factor growth plots show that CATNLF pressure distributions are expected to transition due to TS in the midchord region at the design condition.
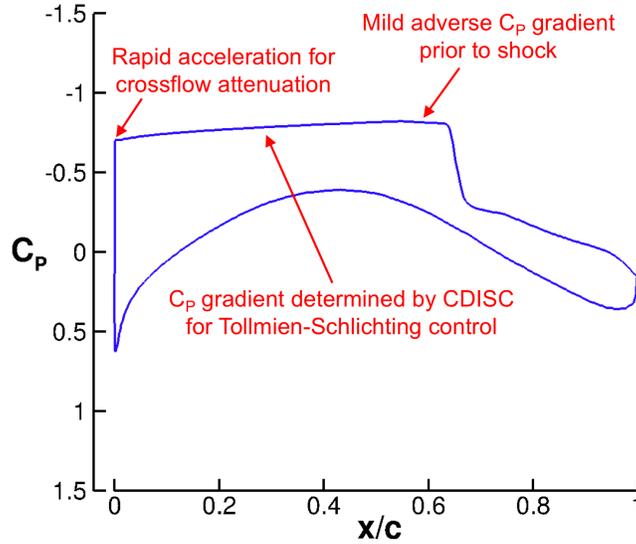
Figure 3. Sample CATNLF pressure distribution for a typical transonic transport with several key features labeled.
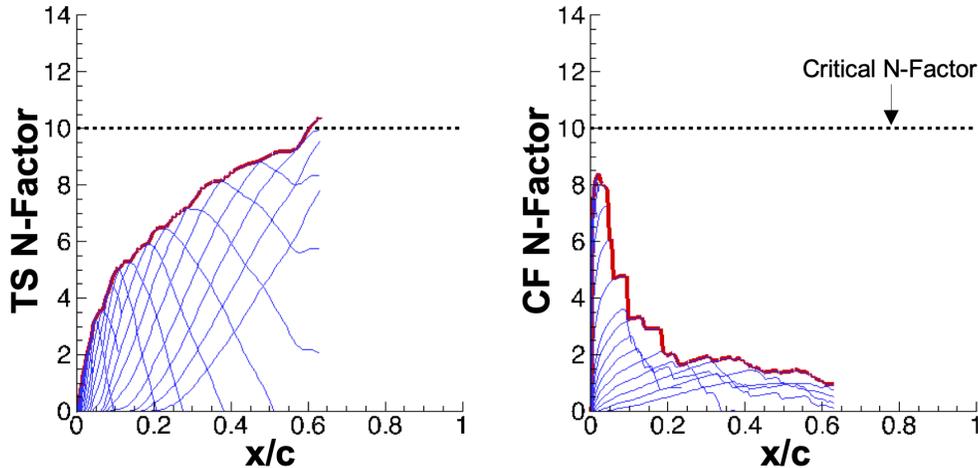

Figure 4. N-factor growth for both TS (left) and CF (right) for the sample CATNLF pressure distribution seen in Figure 3.

III. CATNLF Flight Test Article Design Results

The primary goal of the flight test effort is to experimentally investigate the CATNLF transition delay method in a flight environment. The FATCAT test article has been computationally designed using the tools and methods described previously. This subsection will cover the results of the design, including airfoil shapes, pressure distributions, and predicted extents of laminar flow. The abstract includes only a sample of the design condition results, the final paper will include the finalized geometry, as well as some off-design results.

A. Design Condition Results

The FATCAT flight test article is designed to be as representative as possible of a typical transonic transport wing, which motivated the test article geometry and design conditions selected for this work. As mentioned, FATCAT will be flown attached to the CLIP underneath an F-15B aircraft, as shown in Figure 5. FATCAT was sized to have a leading-edge sweep of 35 deg. and to maximize the test article chord length subject to mounting restrictions and ground clearance requirements. The baseline planform geometry is shown in Figure 6 with reference parameters listed in Table 1. The design flight condition was chosen based on the F-15B flying at an altitude of 5,000 ft at Mach 0.85. This flight condition creates a mean aerodynamic chord Reynolds number of 31 million on the test article at the design

point. The FATCAT test article is designed to be loaded similar to a transonic transport, with a sectional lift coefficient targeted around 0.5. Laminar flow is only targeted for the upper surface, or suction side, on this test article.
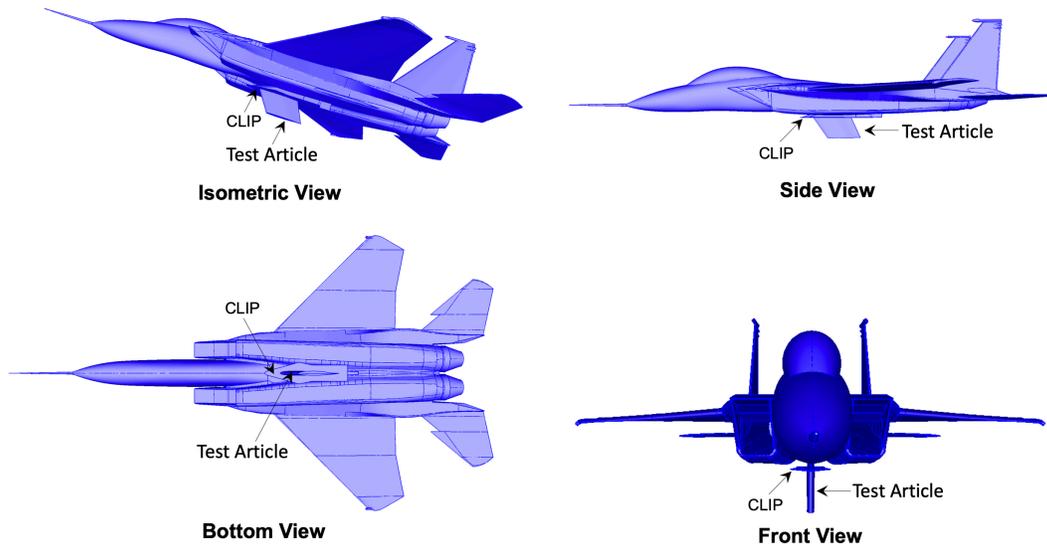

Figure 5. Flight test configuration showing the test article attached to the bottom of the F-15B via the CLIP.
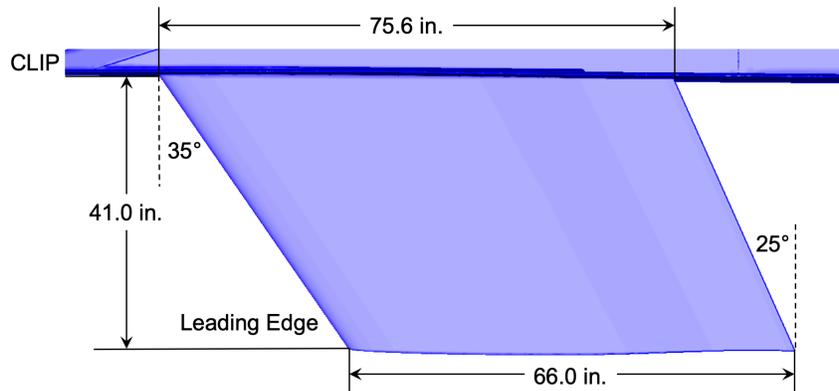

Figure 6. Test article baseline planform shape with dimensions.

**Table 1. Reference parameters and design flight conditions for the FATCAT test article.**

Mean Aerodynamic Chord (ft)	5.9
Root Chord (ft)	6.3
Tip Chord (ft)	5.5
Span (ft)	3.4
Reference Area (ft^2)	19.7
Leading-edge Sweep (deg)	35
Trailing-edge Sweep (deg)	25
Max Thickness	10% chord
Design Mach*	0.85
Design C_L	0.50
Design Altitude (ft)	5,000
Design Re_{MAC} (x10^6)	31.0
Design Re' (x10^6 /ft)	5.3
Design Critical N-factor	10

*Mach measured by the F-15

The FATCAT flight test article will be flown underneath an F-15B aircraft attached to the CLIP. Due to the complexity of the F-15B and CLIP geometry, it was advantageous to simplify the modeled configuration to reduce computational time and resources needed for the design of the flight test article. Two flow solver grids were generated for this work to allow for a more efficient design process. The first grid modeled the entire configuration that will be tested in flight, including the fullspan F-15B with CLIP and test article as seen in Figure 7, and is referred to as the Full Configuration (FC) grid. A second grid was generated with only the FATCAT test article, referred to as the Isolated Test Article (ITA) grid, and is shown in Figure 8.
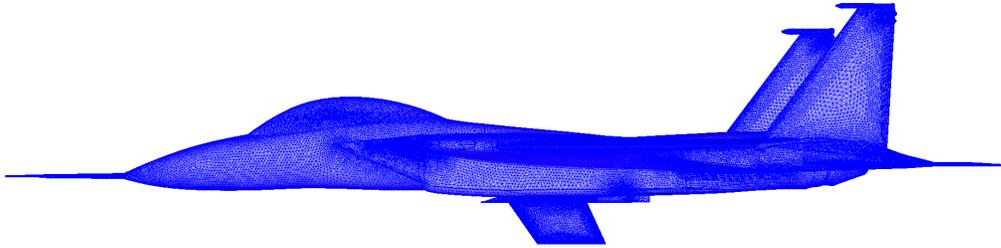
Figure 7. Full Configuration (FC) grid which models the entire flight test configuration, including the fullspan F-15B, CLIP, and test article.
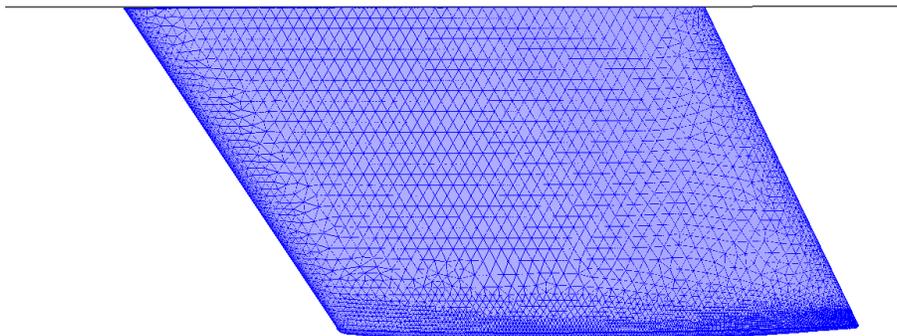
Figure 8. Isolated Test Article (ITA) grid which models only the test article.

The ITA grid is used primarily in the initial design process to do the majority of the reshaping needed to obtain laminar flow. The FC grid is used to do the final adjustments on the shape to account for any influence of the F-15B and CLIP that is expected during flight testing. Initial flow solutions comparing the ITA and the FC results showed the influence of the F-15B and CLIP imposes a local Mach and angle of attack shift on the test article. The Mach and angle of attack shifts, as described in the equations below, were used during the design process on the ITA grid. The fin-like orientation of the test article when mounted on the F-15B (seen in Figure 7) means that an aircraft side slip angle in the FC grid (β_{FC}) equates to a test article angle of attack in the ITA grid (α_{ITA}).

$$M_{ITA} = M_{FC} + 0.02 \qquad\qquad (Eqn. 1)$$

$$\alpha_{ITA} = \beta_{FC} + 2 \text{ deg.} \qquad\qquad (Eqn. 2)$$

The primary objective of this flight test effort is to experimentally validate the CATNLF transition delay method in a flight environment. The transition delay method, as described in the previous subsection, utilizes pressure distributions to suppress the leading-edge CF growth to a subcritical level and grow TS gradually such that it reaches the designated critical N-factor at a specified transition location. For this work, a critical N-factor of 10 is used for both CF and TS to represent a flight environment. On a standard transonic transport, it would likely be desirable to

American Institute of Aeronautics and Astronautics

extend the region of laminar flow as far aft as possible, typically to just ahead of the shock, in order to maximize the drag reduction available to laminar flow technology. However, for the research objectives of this flight test effort, it is advantageous to observe a transition front that is not shock limited (i.e., transitions due to TS reaching a critical N-factor rather than transitioning due to a strong pressure gradient or shock). A non-shock-limited TS transition front is expected to move aft as the flight Reynolds number is reduced due to the N-factor suppression that occurs at lower Reynolds numbers. However, if transition is caused by a shock at the highest Reynolds number, reducing the Reynolds number during flight testing would show little or no difference in the transition location. A design strategy was derived in an attempt to balance the objectives of maximizing the extents of laminar flow, while also characterizing both CF and TS transition in a flight environment. This design strategy aims to have the inboard region of test article maintain laminar flow as far aft as possible, while the outboard region of the test article gradually moves TS transition closer to the leading edge at the design Reynolds number. The inboard portion with an aft transition location will allow for high transition Reynolds numbers to be observed on the test article. The outboard portion with a more forward transition location will enable characterization of Reynolds number effects on laminar flow extents, as well as allow determining the TS critical N-factor experienced in the flight environment. The target transition front using this design strategy is shown in Figure 9, illustrating the notional progression of the transition location with decreasing Reynolds number.
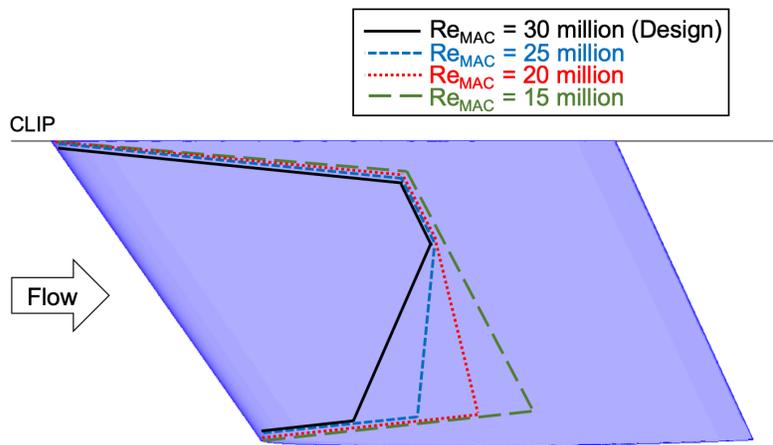

Figure 9. Planform view of the test article with notional transition fronts at different Reynolds numbers illustrating the transition design strategy.

The FATCAT test article is designed using 6 design stations, as shown in the planform view in Figure 10. The baseline geometry was generated using generic supercritical airfoils. The baseline test article showed strong shocks emanating from the leading edge of the root and tip. To alleviate these shocks, the leading-edge planform of the inboard 5 inches and outboard 5 inches were rounded as illustrated in Figure 10. The optimum planform shape to alleviate the shocks is still being explored and will be updated in the final paper. The inboard reduction of leading-edge sweep also helps address attachment line contamination by reducing the Reynolds number based on attachment line momentum thickness (Re_θ) low enough to relaminarize the turbulent attachment line. This method of reducing leading-edge sweep to address attachment line contamination was successfully demonstrated on the previous CRM-NLF wind tunnel model [8, 9].
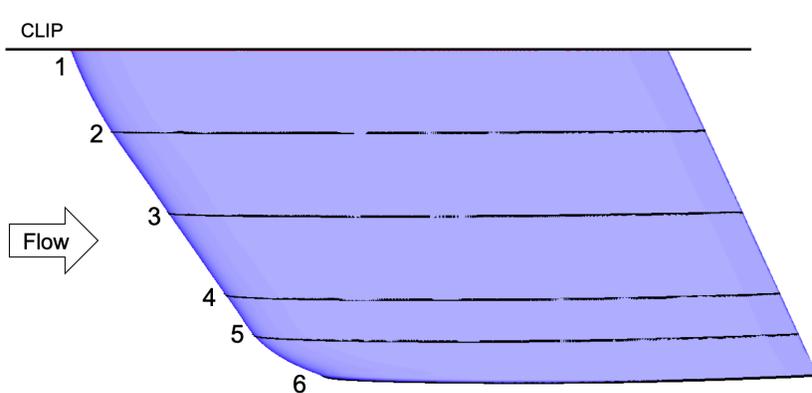
Figure 10. Planform view of the test article with the 6 design stations labeled and illustrating the proposed planform shape changes (inboard and outboard rounding).

The design of the test article is still being finalized, but a sample of the current design shape is included in this abstract. This sample is representative of the type of shape changes needed to obtain the desired pressure distributions. As mentioned previously, the design is first performed on the ITA grid to conserve computational resources, so results in this abstract are from computations on the ITA grid. Figure 11 shows the pressure distribution at design station 3, which is located halfway out the span of the test article. The figure includes the analysis pressures from the baseline airfoil shapes, as well as the new designed airfoil shapes. The target pressure distribution is also shown, which is the CATNLF pressure distribution that CDISC is using to drive the airfoil shape changes. The close match between the design and target pressures illustrates that the shape changes incorporated were effective at obtaining the desired CATNLF pressure architecture. Figure 12 shows the shape changes needed to obtain this CATNLF pressure distribution by comparing the baseline airfoil to the design airfoil. The local twist has been removed from the airfoils to more clearly show the shape changes. There is a notable reduction in leading-edge radius for the design airfoil, as well as a redistribution of camber and thickness. The maximum thickness of 10% chord has been held constant. The N-factor growth that corresponds to the design and target pressure distributions are shown in Figure 13. The CF N-factor curves show that the design has slightly higher CF growth than the target, due primarily to the mismatch in pressure distribution in the leading-edge region, but that both the target and design CF would remain subcritical over the airfoil. This stability analysis shows that the design pressure distribution is predicted to support laminar flow until approximately 45% chord, where it is expected to transition due to TS.
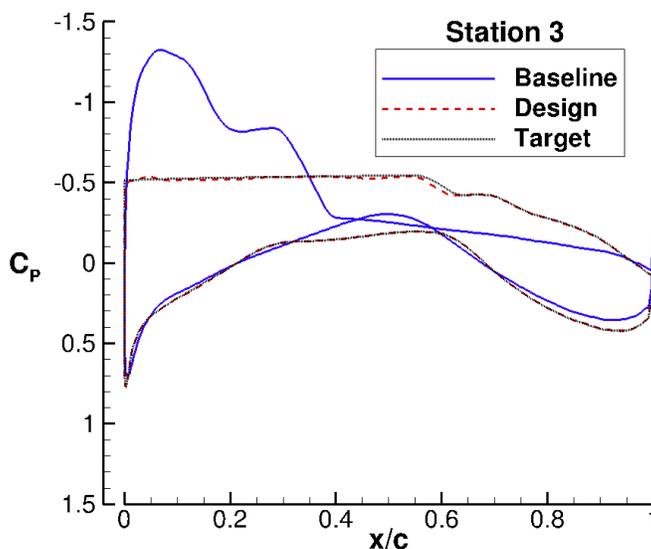
Figure 11. Sample design case at design station 3 comparing the baseline (blue, solid), design (red, dashed), and target (black, dotted) pressures.
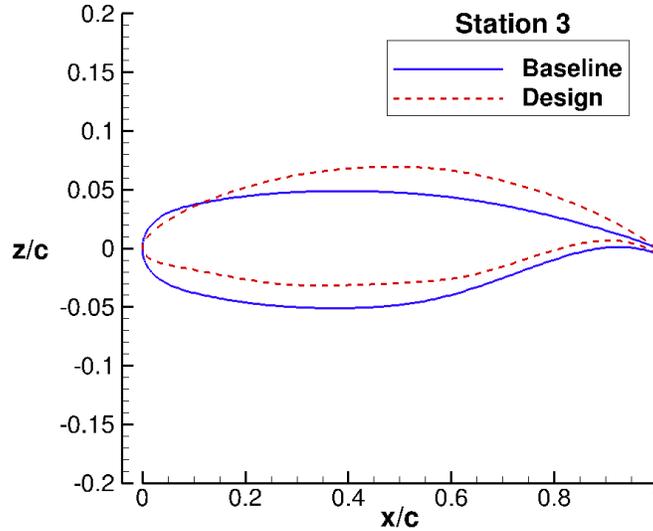
American Institute of Aeronautics and Astronautics

Figure 12. Airfoil shapes with local twist removed for a sample design case at design station 3 comparing the baseline (blue, solid) and the design (red, dashed).
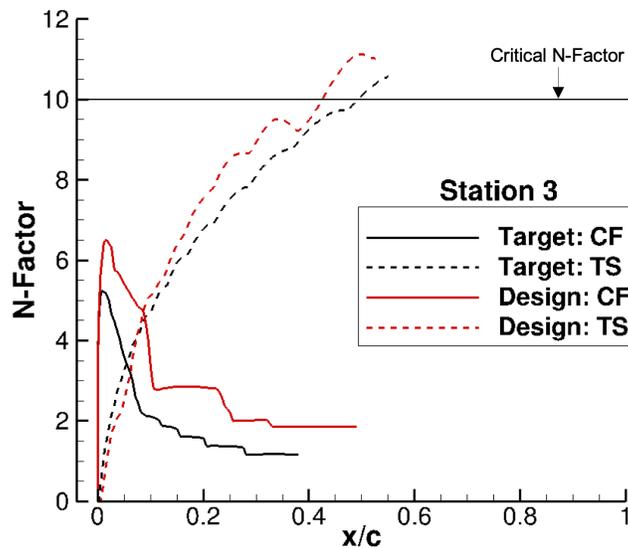

Figure 13. N-factor growth for both CF (solid) and TS (dashed) from the target (black) and design (red) pressure distributions shown in Figure 11.

The airfoils and planform shape changes determined using the ITA grid will be plugged into the FC grid. Another round of design will take place on the FC grid if necessary to ensure the aerodynamic influence of the F-15B is accounted for. The final paper will include airfoil and pressure distributions comparing the ITA design to the FC design. Once the design is finalized, additional design-point analysis will be conducted to be included in the full paper, such as predicted transition fronts and attachment line Re_θ distributions.

B. Off-Design Results
    The paper will include results from several off-design analyses on the finalized flight test article. This will primarily focus on an assessment of laminar flow extents with changing angle of attack and Reynolds number.

IV.   Testing Strategy for Flight Test Article
    The FATCAT flight test article shape is aerodynamically designed to evaluate the CATNLF transition delay method in a flight environment underneath the F-15B testbed. The flight conditions and data acquired for the

experimental investigation will be chosen such that two primary goals can be evaluated. This subsection will include information on these two primary goals, including the motivation, test conditions, and planned FATCAT instrumentation that will help evaluate these goals.

The primary goal of the FATCAT flight test article is to confirm the effectiveness of the CATNLF method in attenuating crossflow growth on a representative transonic transport wing. The wing was designed to be as similar to a transonic transport wing as possible given the size constraints the testbed imposed on the test article. As discussed previously, the test article is a lifting surface with supercritical airfoils and has 35 deg. leading-edge sweep. In order to evaluate the crossflow attenuation strategy, the test article will be tested at low altitudes to produce high mean aerodynamic chord Reynolds numbers (Re_{MAC}). Crossflow growth is strongly correlated to Reynolds numbers, so the high Re_{MAC} values are needed to better represent the typical crossflow growth on a transonic transport. For this test, the Re_{MAC} used to evaluate the CATNLF transition delay method will be between 25 and 31 million, as seen in Table 2.

Due to the test article size limitations imposed by the testbed, relatively high unit Reynolds numbers (Re') are needed in order to obtain these transport-relevant Re_{MAC}. Since bypass transition and transition related to surface roughness are directly correlated to Re', it was advantageous to establish a secondary goal to investigate surface requirements needed at transport-relevant Re'. For this secondary goal, Re' values ranging from 1.0 to 3.4 million/ft will be tested (shown in Table 2), which covers the Re' range seen on current transport aircraft such as the B737 and B777. The method for evaluating surface requirements is still being finalized, but current proposals include incrementally roughening the surface and/or adding known-height imperfections, and studying the impact on laminar flow extents.

Table 2. Test conditions for the two primary goals of the FATCAT test article.

Goal	Transport-relevant Re_{MAC} for CATNLF evaluation		Transport-relevant Re' for surface finish requirements evaluation		
Altitude (ft)	5,000*	12,500	19,600	28,500	49,500
M_{F-15}	0.85 +/- 0.01	0.85	0.85	0.85	0.85
β_{F-15} (deg)	+/- 1.0	+/- 1.0	+/- 1.0	+/- 1.0	+/- 1.0
Re' ($\times 10^6$/ft)	5.3	4.2	3.4	2.6	1.0
Re_{MAC} ($\times 10^6$)	31.0	25.0	20.1	15.1	6.1

*FATCAT test article design condition

The FATCAT test article will be manufactured with several instrumentation capabilities to enable the successful evaluation of the two primary goals. The primary source of data for this test is transition visualization data, which will be acquired via an existing infrared (IR) camera system attached to the F-15B that views the righthand (suction) surface of the test article. To improve the quality of this transition visualization data, a carbon-based resistive heating layer will be used to provide the required temperature gradient used to visualize laminar flow. This heating layer was experimentally validated in both the CRM-NLF wind tunnel test and the ReHEAT flight test [17]. Another key source of data for this flight test is the surface pressure data, which will confirm that the CATNLF pressure architecture is obtained on the flight test article. Chordwise static pressure orifices will be manufactured into the model at 2-3 spanwise stations to acquire this data. Subsurface thermocouples are also planned to be incorporated into the model to provide surface temperature data along chordwise distributions at 2-3 spanwise stations. Additionally, the test article will likely have a series of flush-mounted Kulites for unsteady shock and crossflow data. A trailing edge boundary layer rake has been discussed to evaluate aft-wing flow separation, and attachment line boundary layer data may be obtained via leading-edge Preston tubes. The test article instrumentation is still being finalized, and will be updated in the final paper.

It has been proposed that the FATCAT flight test article be tested in a wind tunnel to provide a direct comparison of laminar flow extents in two environments. This will likely take place in the National Transonic Facility at the NASA Langley Research Center after the flight test effort. Additional detail on this plan, including predictions of laminar flow extents of the FATCAT test article in a wind tunnel environment, will be included in the final paper.

V. Concluding Remarks

The CATNLF boundary layer transition delay method was developed to provide significant drag reduction on transport aircraft through enabling natural laminar flow on wings with high sweep. Sustaining laminar flow on these wings has presently been limited by the growth of crossflow instabilities very near the leading edge that is common on components with high sweep at high Reynolds numbers. The CATNLF transition delay method uses carefully

designed airfoils to provide specific pressure architecture that attenuates the crossflow in the leading-edge region and tailors the Tollmien-Schlichting growth to delay transition to a designated chordwise location. The method was experimentally investigated in the wind tunnel test of the CRM-NLF in 2018, and positive results from that wind tunnel test has led to a flight test series to evaluate the CATNLF concept in a flight environment. The flight test series is comprised of three flights to be tested on an existing testbed underneath an F-15B, each with unique test hardware to support the test objectives. This abstract aims to document the aerodynamic design of the test article used in the third flight of the series. The test article, referred to as FATCAT, is designed to represent a typical transonic transport wing using the CATNLF design method. The final geometry of FATCAT is still being finalized; the final paper will include the completed geometry and associated analysis. The design was performed, flight matrix selected, and instrumentation chosen with the two primary test goals in mind: to confirm the effectiveness of the CATNLF method in attenuating crossflow growth on a representative transonic transport wing, and to investigate surface requirements needed at transport-relevant unit Reynolds numbers.

Acknowledgments

References

[1] Boeing Company, "Commercial Market Outlook 2019 – 2038", Website Accessed October 2019, [https://www.boeing.com/resources/boeingdotcom/commercial/market/commercial-market-outlook/assets/downloads/cmo-sept-2019-report-final.pdf].

[2] Norris, G., "Picture: Boeing plans plain grey natural laminar flow nacelles for 787s in bid to reduce fuel burn", Flight International, 11 July, 2006. https://www.flightglobal.com/news/articles/picture-boeing-plans-plain-grey-natural-laminar-flow-nacelles-for-787s-in-bid-to-reduce-fuel-207769/

[3] Fujino, M., "Design and Development of the HondaJet", AIAA International Air and Space Symposium and Exposition: The Next 100 Years, AIAA 2003-2530, July 2003.

[4] Saric, William S.; Carrillo, Ruben, B., Jr.; and Reibert, Mark S.: Leading-Edge Roughness as a Transition Control Mechanism. AIAA 1998-0781, January 1998.

[5] Campbell, R. L., and Lynde, M. N., "Natural Laminar Flow Design for Wings with Moderate Sweep", 34th AIAA Applied Aerodynamic Conference, AIAA AVIATION Forum, AIAA 2016-4326, June 2016.

[6] Lynde, M. N. and Campbell, R. L., "Expanding the Natural Laminar Flow Boundary for Supersonic Transports", 34th AIAA Applied Aerodynamic Conference, AIAA AVIATION Forum, AIAA 2016-4327, June 2016.

[7] Lynde, M. N., and Campbell, R. L., "Computational Design and Analysis of a Transonic Natural Laminar Flow Wing for a Wind Tunnel Model," AIAA-2017-3058, June 2017.

[8] Lynde, M. N., Campbell, R. L., and Viken, S. A., "Additional Findings from the Common Research Model Natural Laminar Flow Wind Tunnel Test (Invited)," AIAA-2019-3292, June 2019.

[9] Lynde, M. N., Campbell, R. L., Rivers, M. B., Viken, S. A., Chan, D. T., Watkins, A. N., and Goodliff, S. L., "Preliminary Results from an Experimental Assessment of a Natural Laminar Flow Design Method", AIAA 2019-2298, January 2019.

[10] Rivers, M., Lynde, M., Campbell, R., Viken, S., Chan, D., Watkins, A., and Goodliff, S., "Experimental Investigation of the NASA Common Research Model with a Natural Laminar Flow Wing in the NASA Langley National Transonic Facility", AIAA 2019-2189, January 2019.

[11] Malik, M.R., Crouch, J.D., Saric, W.S., Lin, J.C., and Whalen, E.A., "Application of Drag Reduction Techniques to Transport Aircraft", Encyclopedia of Aerospace Engineering, 2015.

[12] Owens, L., Beeler, G., King, R., Chou, A., Balakumar, P., and Banks, D., "Supersonic Crossflow Transition Control in Ground and Flight Tests", AIAA 2019-1651, January 2019.

[13] Frink, N.T., Pirzadeh, S.Z., Parikh, P.C., Pandya, M.J., and Bhat, M.K., "The NASA Tetrahedral Unstructured Software System," The Aeronautical Journal, Vol. 104, No. 1040, October 2000, pp.491-499.

[14] Campbell, R. L., "Efficient Viscous Design of Realistic Aircraft Configurations," AIAA-98-2539, June 1998.

[15] Wie, Y.-S., "BLSTA: A Boundary Layer Code for Stability Analysis," NASA CR 4481, 1992.

[16] Chang, C.-L., "The Langley Stability and Transition Analysis Code (LASTRAC): LST, Linear and Nonlinear PSE for 2-D, Axisymmetric, and Infinite Swept Wing Boundary Layers," AIAA 2003-0974, 2003.

[17] Watkins, A.N., Goodman, K.Z., and Peak, S.M., "Transition Detection at Cryogenic Temperatures Using a Carbon-Based Resistive Heating Layer Coupled with Temperature Sensitive Paint", AIAA 2019-2191, January 2019.